Interface Microstructure and Strength Properties of the Diffusion-Bonded Joints of Titanium | Cu Interlayer | Stainless Steel

S. KUNDU, S. CHATTERJEE, D. OLSON, and B. MISHRA

In the present study, copper was used as an intermediate material in diffusion bonding between titanium and stainless steel. The process was carried out in the temperature range of 850 °C to 1000 °C for 60 minutes and at 900 °C for 30 to 150 minutes under the compressive stress of 3 MPa in a vacuum. The effects of temperature and time on the microstructure of Ti | Cu | stainless steel diffusion-bonded joints were studied. The interface microstructures of the bonded assemblies were observed in optical and scanning electron microscopes and an electron probe microanalyzer. Formation of various types of reaction products near the interface was detected using the X-ray diffraction technique. The maximum tensile and shear strength of ~101 pct of that of Ti and of ~86 pct of that of Ti, respectively, along with ~8.5 pct elongation, were obtained at 900 °C for 60 minutes. Observation of fracture surfaces demonstrates that failure takes place through the SS-Cu interface.

I. INTRODUCTION

IN recent years, nuclear and chemical processing industries strongly demanded transition joints between titanium/titanium alloy and stainless steel for application in service.[1,2] The diffusion bonding technique provides a near-net-shape forming process for similar and dissimilar materials without gross macroscopic distortion and with minimum dimensional tolerances.[3] These two materials, when joined by conventional fusion welding, result in segregation of chemical species, stress concentration sites, and formation of intermetallic phases near the interface of the joint due to the very low solubility of Ti and Fe at room temperature.[4]

The literature reports that joints produced by direct bonding between Ti and stainless steel showed the formation of Cr, Fe, and Ti base reaction products.[5–8] Aleman et al.[6] reports that the TEM studies on titanium-306 stainless steel diffusion-bonded joints indicated the formation of σ, Fe_2Ti, $FeTi$, λ, Fe_2Ti_4O, and TiC in the diffusion interface. Ghosh et al.[7] report that solid-state diffusion bonding was carried out between titanium and stainless steel and achieved a maximum tensile strength of 222.1 ± 9 MPa when processed at 850 °C for 90 minutes and also report that bond strength drops with a rise in bonding temperature due to the increase in the width of intermetallic phases at the diffusion zone. Copper can also be considered as a useful intermediate material to reduce the bonding parameters (i.e., temperature and time) due to its low melting point with respect to Fe, Cr, Ni, and Ti. An increase in the transportation of atoms of these elements at higher temperature (>0.5 T_m, with T_m melting point in K) will encourage a good contact between the mating surfaces. Moreover, copper does not form any intermetallic phases with iron. The Cu-Ti binary phase diagram shows the occurrence of Cu_2Ti, Cu_3Ti_2, $CuTi$, and $CuTi_2$ with increasing Cu content.[8] Eroglu et al. also report that the Cu-Ti base intermetallic phases have higher plasticity than the Fe-Ti base intermetallic phase.[9] In the previous attempt, nickel was used as an intermediate material for the same diffusion couple and the bond tensile and shear strengths of 311 and 236 MPa, respectively, were obtained due to the absence of Fe-Ti and Fe-Cr-Ti base intermetallic compounds.[10]

The present investigation reports diffusion bonding of commercially pure titanium and 304 stainless steel using copper as an interlayer at various temperatures and times in vacuum. The effect of bonding temperature and time on microstructure and mechanical properties has been investigated.

II. EXPERIMENTAL PROCEDURE

The chemical compositions and room-temperature mechanical properties of commercially pure titanium and 304 stainless steel are given in Tables I and II, respectively. Both of them were received in the form of rod having 20-mm diameter. From the base materials, cylinders of 15-mm diameter × 30-mm length were machined.

The mating surfaces of the cylinders were prepared by conventional grinding and polishing techniques by final

S. KUNDU, Research Associate, and S. CHATTERJEE, Professor and Head, are with the Department of Metallurgy and Materials Engineering, Bengal Engineering and Science University, Shibpur, Howrah-711103, India. D. OLSON and B. MISHRA, Professors, are with the Department of Metallurgical and Materials Engineering, Colorado School of Mines, Golden, CO 80401. Contact e-mail: bmishra@mines.edu

Table I. Chemical Compositions of the Base Metals (Weight Percent)

Alloy	C	Fe	Ti	Mn	Si	S	P	Cr	Ni	O	N	H
Ti	0.02	0.10	bal	—	—	—	—	—	—	0.15	0.02	0.0011
SS	0.06	bal	—	1.38	0.37	0.013	0.03	18.15	8.50	—	0.005	—

Table II. Mechanical Properties of the Base Metals at Room Temperature

Alloy	Shear Strength (MPa)	0.2 Pct Yield Stress (MPa)	Ultimate Tensile Strength (MPa)	Fracture Elongation (Pct)
Ti	296.6	205	319	23
SS	573.0	740	822.5	42

polishing with 1-μm diamond paste. The copper foil of 300-μm thickness and 99.95 pct purity was used as an intermediate material, and both the surfaces of the interlayer were polished in the same fashion. The mating surfaces were cleaned in acetone and dried in air. The Ti | Cu | SS assembly was kept in contact in a fixture and was inserted in a vacuum chamber. The diffusion bonding was carried out in the temperature range of 850 °C to 1000 °C in steps of 50 °C for 60 minutes and 900 °C for 30 to 150 minutes in steps of 30 minutes in (6 to 8) × 10^{-4} Pa vacuum. The compressive stress of 3 MPa was applied along the longitudinal direction of the sample, and the stress was measured at room temperature. Heating was done at the rate of 0.24 °C s^{-1} at the time of processing, and after the operation, the samples were allowed to cool in vacuum at a cooling rate of 0.1 °C s^{-1} up to 300 °C.

The diffusion bonded joints thus formed were cut longitudinally and prepared by conventional techniques for metallographic observations. The titanium side was etched in an aqueous solution of 88 mL H_2O, 4 mL HF, and 8 mL HNO_3. The stainless steel side was etched by a mixture of 10 mL HNO_3, 40 mL HCl, and 50 mL glycerol. A solution containing 5 g $FeCl_3$, 2 mL HCl, and 96 mL ethanol was used for etching pure copper. The structural change owing to diffusion was observed in a light microscope (Correct SDME TR5, Seiwa Optical Co. Ltd, Makaro-Ku, Tokyo, Japan). Polished samples were also examined in a scanning electron microscope (JEOL* JXA 840A) using backscattered

*JEOL is a trademark of Japan Electron Optics Ltd., Tokyo.

mode (SEM-BSE) to reveal the reaction layers near the diffusion-bonded interface. The compositions of the reaction layers were determined in atomic percent using an electron probe microanalyzer (Cameca Sx 100). The presence of intermetallic phases in the reaction zone was confirmed by X-ray diffraction study (PHILIPS** PW

**PHILIPS is a trademark of Philips Electronic Instruments Corp., Mahwah, NJ.

1840) on the fracture surfaces of the couples using a copper target. The scanning span of 20 to 80 deg with a step size of 0.02 deg (=2θ) was used during this

investigation. Tensile properties of the transition joints were evaluated in a tensile testing machine (Instron 4204) at a crosshead speed of 8.33 × 10^{-4} mm s^{-1} at room temperature. Cylindrical tensile specimens were machined per ASTM specification (vol.03.01 E8M-96) with a gage diameter and length of 4 and 20 mm, respectively. The interlayer was at the center of the gage length. The shear strength of the bonded joints was evaluated at room temperature using a screw tensile testing machine set at a crosshead speed of 8.3 × 10^{-3} mm s^{-1}.[9] The shear test specimens were machined to a diameter of 10 mm. Four samples were tested at each processing parameter. The microhardness along the cross section of the diffusion-bonded joints was determined by a microhardness tester. A dwelling time of 20 seconds and a 10-g load were used for the measurement. Fracture surfaces of the samples were observed in secondary electron mode in SEM (Leica S440, Cambridge, UK) using energy-dispersive spectroscopy (Oxford 5431, High Wycombe, UK) to reveal the nature and location of failure under loading.

III. RESULTS AND DISCUSSION

Optical micrographs of the transition joints are shown in Figure 1. From the micrographs, it can be seen that the diffusion interfaces are free from cracks and interface lines are clearly visible. A thin diffusion layer at the SS-Cu interface was revealed for all the bonding parameters. The Cu-Ti interface is characterized by the presence of a light-shaded reaction zone and the Widmanstätten α-β titanium structure. Copper is a strong β-stabilizing element. The migration of copper atoms to titanium lattice lowers the eutectoid transformation temperature of titanium, and α-β phase aggregate forms due to the decomposition of β-Ti during cooling.[8,10] At all temperatures, copper and stainless steel have a close-packed fcc structure, so the extent of diffusion of these elements across the bond line is limited. The Ti with the two-phase structure, i.e., α(hcp) + β(bcc) at room temperature transforms to β-Ti at 882 °C. Owing to more open atomic arrangement in the bcc matrix, copper atoms can travel a longer distance in titanium lattice than vice versa.[7]

Figures 2 and 3 show the backscattered electron images of the bonded samples. At the SS-Cu interface, layerwise reaction products are observed and their
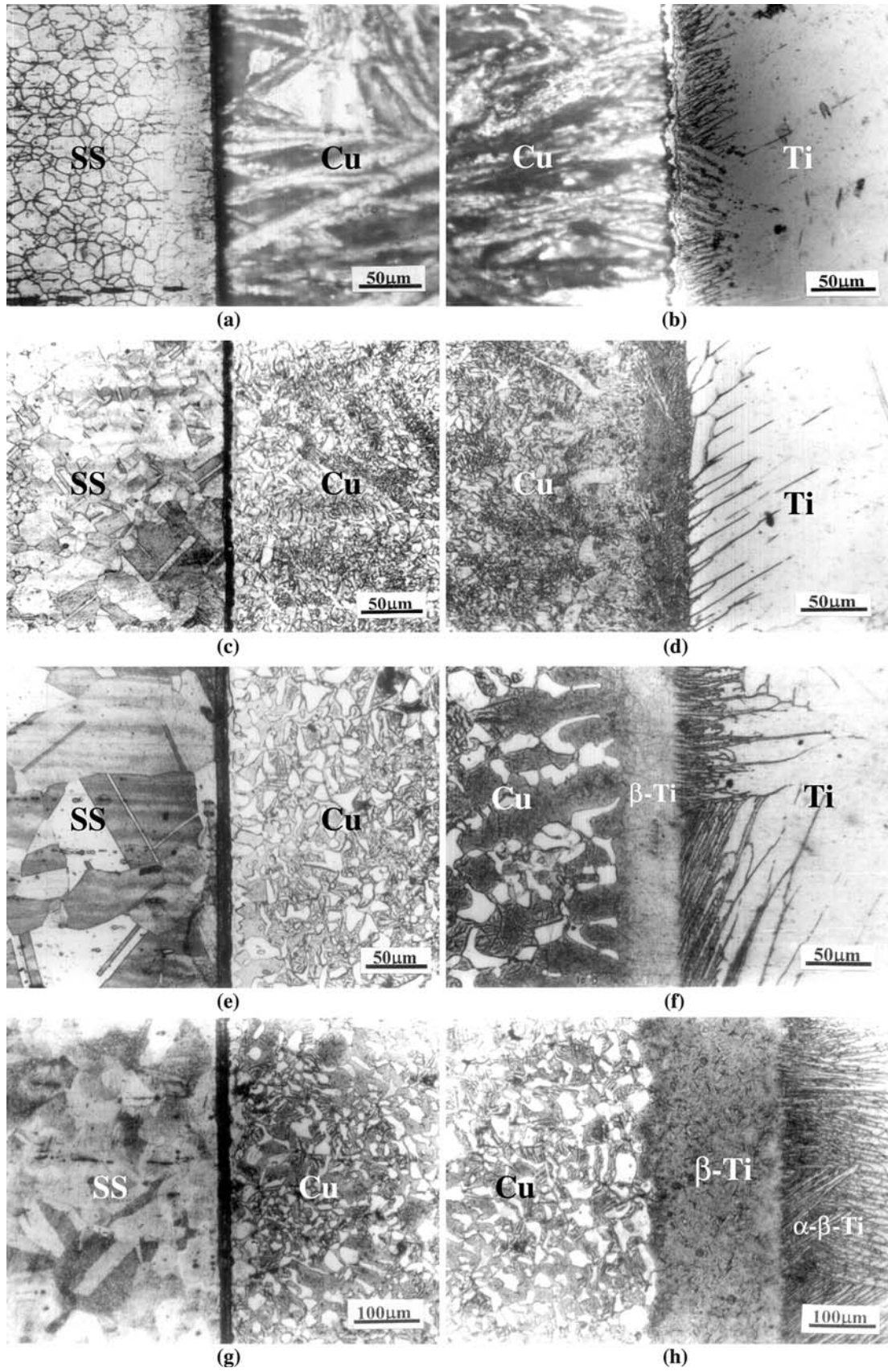
Fig. 1—Optical microstructure of the diffusion-bonded assemblies joined at (*a*) and (*b*) 850 °C for 60 min, (*c*) and (*d*) 900 °C for 60 min, (*e*) and (*f*) 950 °C for 60 min, and (*g*) and (*h*) 900 °C for 150 min.
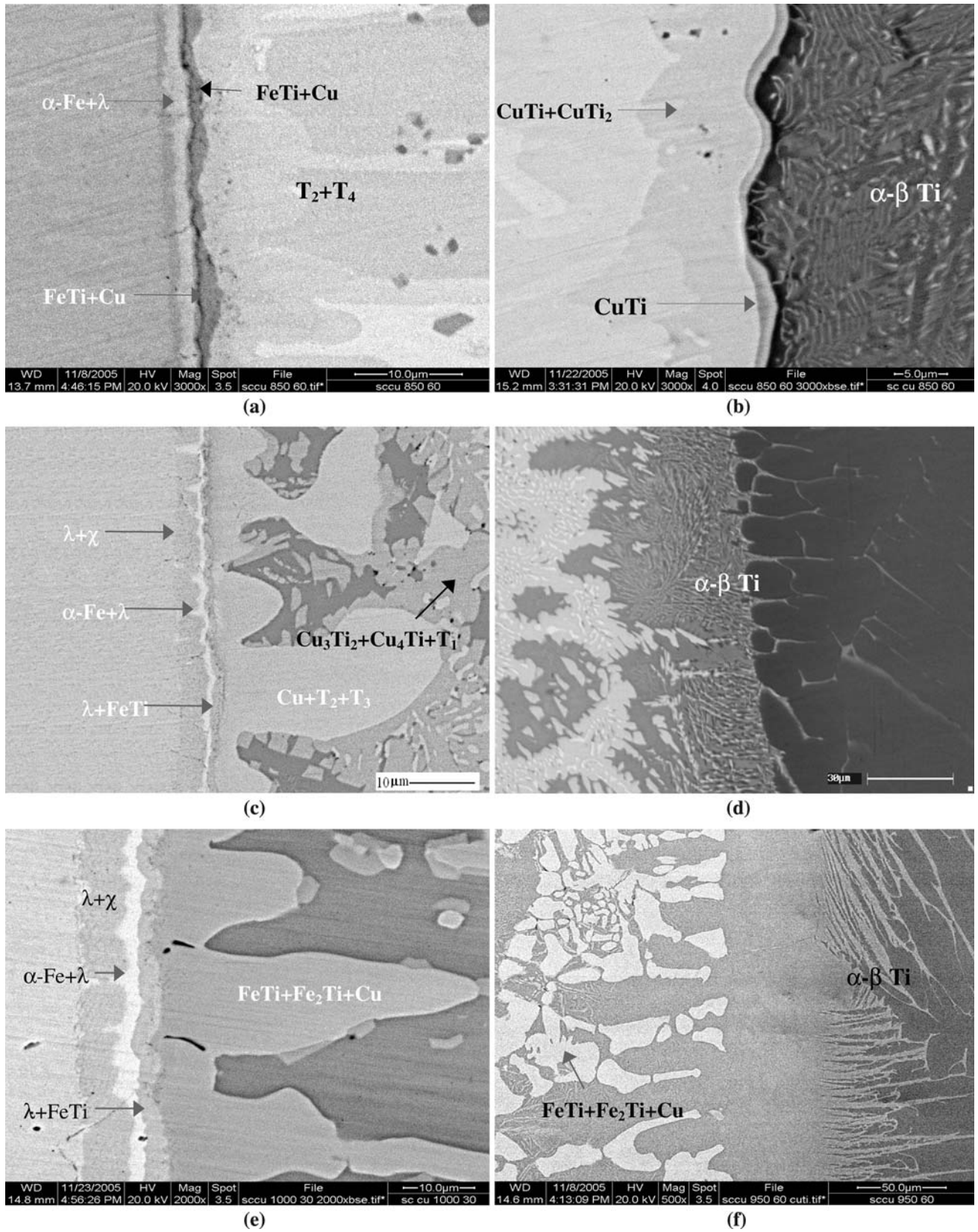
Fig. 2—Backscattered electron image of the specimen processed for 60 min at (*a*) 850 °C, SS-Cu interface; (*b*) 850 °C, Cu-Ti interface; (*c*) 900 °C, SS-Cu interface; (*d*) 900 °C, Cu-Ti interface; (*e*) 950 °C, SS-Cu interface; and (*f*) 950 °C, Cu- Ti Interface.

chemical compositions are given in Table III. The deep-shaded reaction layer is the $\lambda + \chi$ phase mixture near the stainless steel side. Close to the $\lambda + \chi$ phase mixture, the thin bright region is the phase mixture of $\lambda + \alpha$-Fe.[11] The light-shaded layer has been observed next to the $\lambda + \alpha$-Fe phase mixture, which is the $\lambda +$ FeTi phase mixture. At 1000 °C for 60 minutes and at 900 °C for 120 minutes and 150 minutes, these areas contain a $\lambda +$ FeTi $+ \beta$-Ti phase mixture. At 850 °C for 60 minutes and at 900 °C for 30 minutes,

$\lambda + \chi$
FeTi+Fe$_2$Ti+Cu
α-Fe+λ
λ+FeTi+β-Ti
20 μm

(a)

β Ti
α-β Ti
FeTi+Fe$_2$Ti+Cu
100μm

(b)

Fig. 3—Backscattered electron image of the specimen processed at 900 °C for 150 min: (a) SS-Cu interface and (b) Cu-Ti interface.

$\lambda + \chi$ and $\lambda +$ FeTi/$\lambda +$ FeTi $+ \beta$-Ti phase mixtures have not been observed at the SS-Cu interface.

At 850 °C for 60 minutes, the deep-shaded area was observed at the SS-Cu interface in the Cu side, and this is enriched with Ti(~47.3 to 48.9), Cu(~16.5 to 17.2), Fe(~29.4 to 30.1), and a small amount of Cr(~4.1 to 4.5) and Ni(bal). This region is presumably the phase mixture of FeTi + Cu.[12] Beek et al.[13] reported that nearly 38 at. pct Cu can be dissolved in FeTi. The light-shaded area in the copper side consists of Ti(~41.2 to 42.3), Cu(~45.1 to 45.9), Fe(~9.7 to 10.6), Cr(~2.1 to 2.4), and Ni(bal), which is presumably a phase mixture of $T_2 + T_4$. The T_2 phase is Ti$_{40}$Cu$_{60-x}$Fe$_x$; $5 < x < 17$ with structure resembles Ti$_2$Cu$_3$ and T_4 is Ti$_{37}$Cu$_{63-x}$Fe$_x$; $5 < x < 7$.[13] In the Cu-Ti interface (Figure 2(b)), close to copper, the faint area contains Ti(~50.1 to 51.2) and Cu(bal) and corresponds to the CuTi + CuTi$_2$ phase mixture having a thickness of ~8.9 μm. Next to CuTi + CuTi$_2$, the light-shaded reaction band has been observed, which is enriched in Ti(~66.2 to 67.9) and Cu(bal); hence, the Cu-Ti binary phase diagram indicates this as a CuTi phase, which is of ~1.4-μm thickness.[8] The elemental concentration profiles of both interfaces of this bonded sample are given in Figure 4.

At 900 °C for 60 minutes, the shaded and light-shaded areas have been observed at the SS-Cu and at the Cu-Ti interface in the copper side. The shaded reaction area contains Ti(~62.5 to 63.1), Cu(~29.3 to 29.9), and Fe(~6.4 to 6.8) with a small amount of Cr(~0.9 to 1.4) and Ni(bal). The light-shaded area contains Ti(~50.5 to 51.9), Cu(~26.5 to 27.9), Fe(19.7 to 19.9) Cr(~3.1 to 3.5), and Ni(bal). The isothermal Fe-Cu-Ti ternary phase diagram indicates that the shaded and light-shaded areas contain a phase mixture of Cu$_3$Ti$_2$ + Cu$_4$Ti + T_1 and Cu + T_2 + T_3, respectively. The term T_1 is Ti$_{33}$Cu$_{67-x}$Fe$_x$; $1 < x < 2.5$, and T_3 is Ti$_{43}$Cu$_{57-x}$Fe$_x$; $21 < x < 24$, having structure closely related to Ti$_3$Cu$_4$.[13]

At 950 °C and 1000 °C for 60 minutes and at 900 °C for 90 to 150 minutes, both SS-Cu and Cu-Ti interfaces (marked in Figures 2(e) and (f)), the light-shaded area indicates the FeTi + Fe$_2$Ti + Cu phase mixture with a composition of Ti(~53.7 to 54.3), Fe(~24.1 to 25.9), Cu(~16.2 to 17.8), Cr(2.2 to 2.6), and Ni(bal). At 900 °C and 950 °C for 60 minutes, the dark area of β-Ti is observed at the SS-Cu and at the Cu-Ti interfaces (Figures 2(c) through (f)) with a composition of Ti(~84.8 to 86.5), Fe(~6.4 to 7.5), Cr(~2.1 to 2.4), Ni(~0.8 to 1.2), and Cu(~bal) in the Cu side. However, at 1000 °C for 60 minutes and at 900 °C for 90 minutes
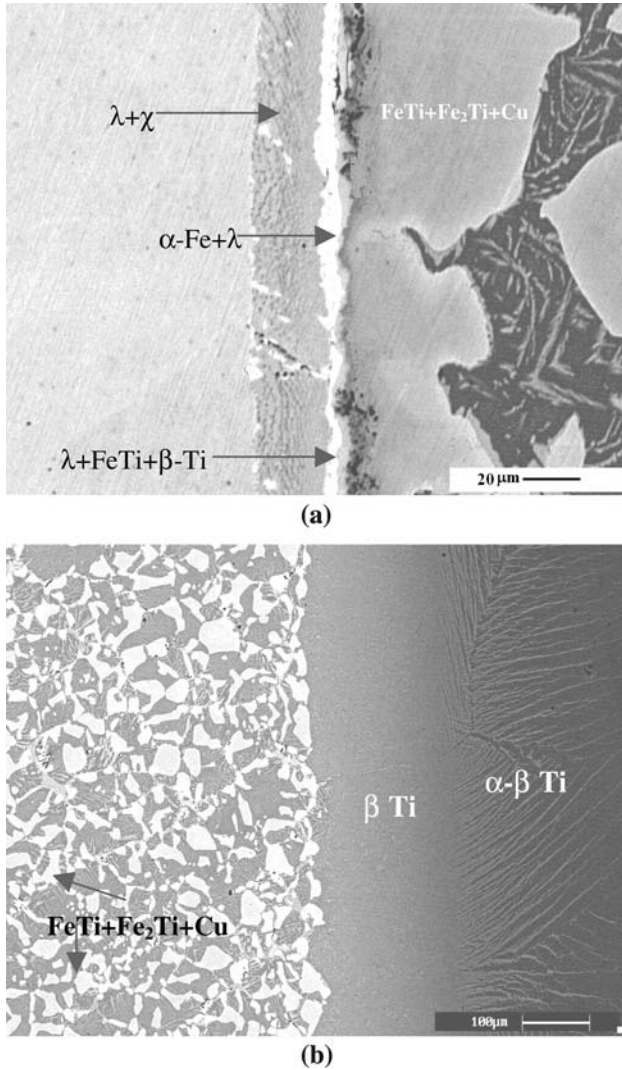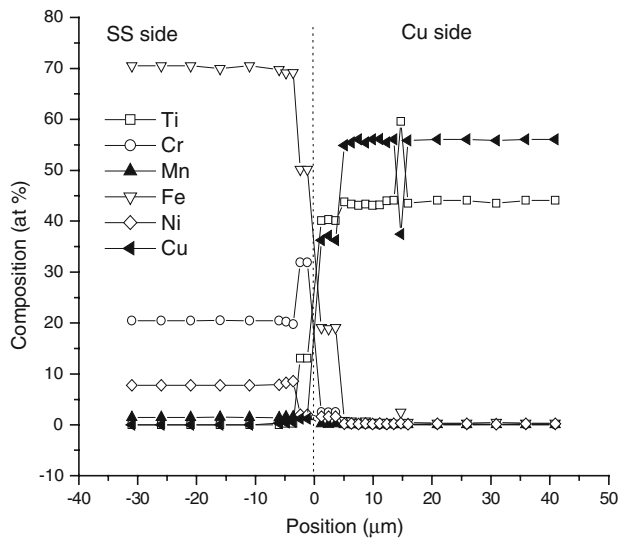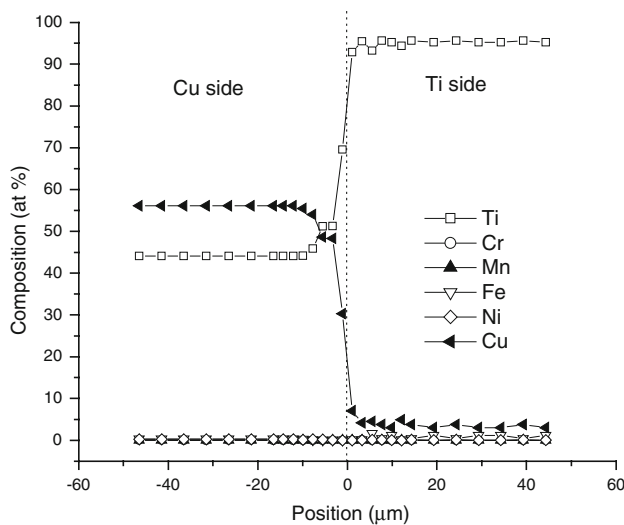
Table III.   EPMA Chemical Analysis of the Bonded Specimen at SS-Cu Interface

	Elements (At. Pct)				
Reaction Products	Fe	Cr	Ni	Cu	Ti
$\lambda + \chi$	61.8 to 63.6	27.0 to 29.6	2.2 to 3.2	bal	3.9 to 5.5
α-Fe + λ	55.6 to 56.34	26.5 to 28.3	2.6 to 3.4	bal	12.8 to 13.7
$\lambda +$ FeTi	46.6 to 49.5	11.2 to 14.3	2.3 to 3.3	bal	32.9 to 35.9
$\lambda +$ FeTi $+ \beta$-Ti	35.6 to 36.9	10.3 to 11.7	3.2 to 3.9	bal	47.1 to 47.9

Fig. 4—EPMA concentration profile of the bonded specimen processed at 850 °C for 60 min: (a) 88-Cu and (b) Cu-Ti interfaces.

and above, this area is FeTi + β-Ti phase mixture with a composition of Ti(~75.8 to 77.5), Fe(~12.9 to 14.8), Cr(~5.6 to 7.2), Ni(~0.8 to 1.3), and Cu(~bal).

At 900 °C for 150 minutes, the microvoids have been observed at the SS-Cu interface (Figure 3(a)) due to the imbalance in mass transfer across the interfaces and generate voids. Orhan et al.[14] and Hinotani et al.[15] reported a similar type of voids for the diffusion couple of microduplex stainless steel/titanium alloy and titanium/nickel, respectively. In the present work, in SEM-BSE images, these discontinuities are not clearly evident at the lower processing parameters due to their finer size.

The diffusion of chemical species is easier through interlayer due to higher migration of copper in the temperature range of 850 °C to 1000 °C for 60 minutes and at 900 °C for 30 to 150 minutes. The Ti can migrate to the stainless steel side and Fe, Cr, and Ni can traverse to the Ti side. Hence, the 300-μm copper interlayer cannot restrict the formation of Fe-Ti and Fe-Ti-Cr base intermetallic phases. The thickness of the reaction products increases with an increase in the bonding temperature and time, and these are given in Tables IV and V.

The X-ray diffraction studies confirmed the presence of different intermetallics in the fracture interfaces and are given in Figure 5. The X-ray diffraction study indicates the occurrence of χ, α-Fe, Cr_2Ti, Fe_2Ti, FeTi, CuTi, Cu_4Ti, Cu_3Ti_2, T_1, T_2, T_3, and β-Ti. The λ phase, which is a solid solution of Fe_2Ti and Cr_2Ti, is identified separately in the X-ray diffraction study. The formation of α-Fe in the stainless steel matrix supports the findings of an earlier investigation, where it has been stated that ~0.8 at. pct of Ti in austenite matrix promotes the formation of bcc ferrite.[16]

The mechanical properties of the diffusion-bonded joints with the change in bonding temperature are shown in Figure 6. It can be seen that when the bonding temperature is 850 °C, the bond strength and breaking strain of the diffusion couple are low due to the incomplete coalescence of the mating surfaces. The presence of voids is even found at 850 °C with the dimension of ~1.1 μm in the fracture surface. At this joining

Table IV. Width of the Reaction Product Formed at the SS-Cu Interface Processed for 60 Minutes

Bonding Temperature (°C)	Width of the Reaction Products in the (SS-Cu) Diffusion Zone (μm)		
850	α-Fe + λ ~ 1.5	FeTi + Cu ~ 1.3	
900	λ + χ ~ 3.6	α-Fe + λ ~ 1.2	λ + FeTi ~ 1.67
950	λ + χ ~ 6.6	α-Fe + λ ~ 3.3	λ + FeTi ~ 3.4
1000	λ + χ ~ 16.2	α-Fe + λ ~ 4.6	λ + FeTi + β-Ti ~ 5.2

Table V. Width of the Reaction Product Formed at the SS-Cu Interface Processed at 900 °C

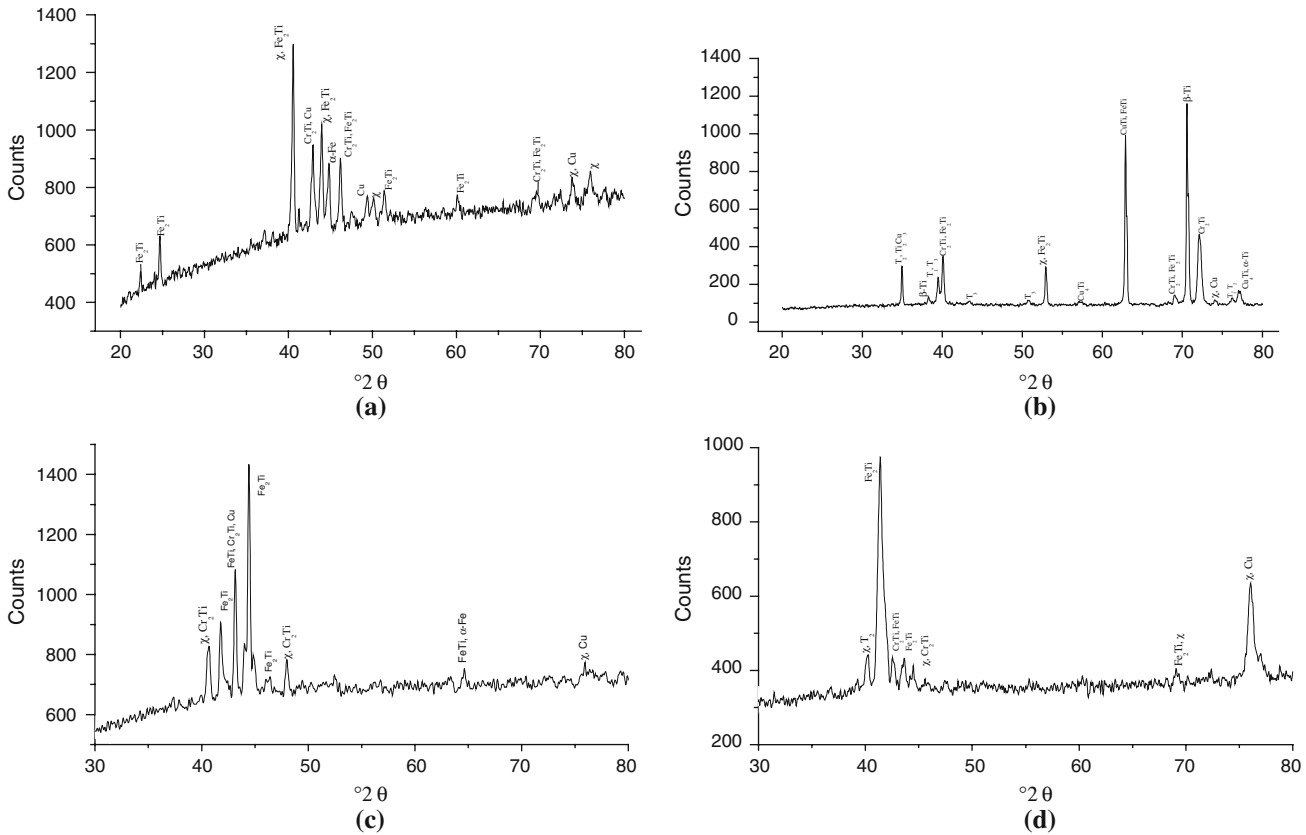| Bonding Time (min)	Width of the Reaction Products in the Diffusion Zone (μm)		
30	α-Fe + λ ~ 1.6	FeTi + Cu ~ 1.6	
60	λ + χ ~ 3.6	α-Fe + λ ~ 1.2	λ + FeTi ~ 1.67
90	λ + χ ~ 5.4	α-Fe + λ ~ 1.3	λ + FeTi ~ 1.72
120	λ + χ ~ 15.9	λ + α-Fe ~ 1.4	λ + FeTi + β-Ti ~ 2.1
150	λ + χ ~ 24.4	λ + α-Fe ~ 6.8	λ + FeTi + β-Ti ~ 3.5

Fig. 5—X-ray diffraction pattern of the fracture surface of the bonded sample processed at 900 °C for (*a*) and (*b*) 60 min; and (*c*) and (*d*) 120 min.
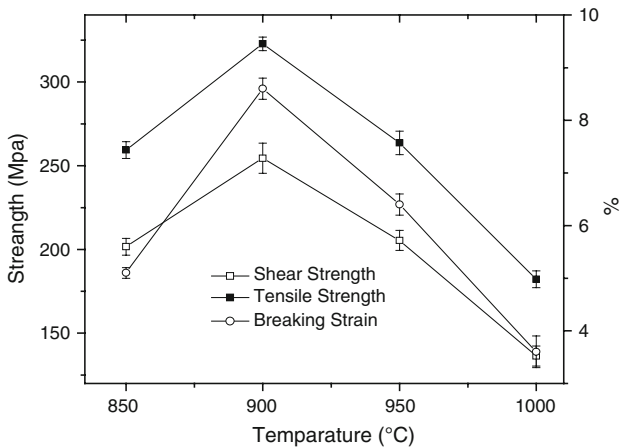

Fig. 6—Mechanical properties of the bonded joints processed for 60 min.

temperature, the migration of copper atoms is substantial. However, the yield strength of base materials still remains high, which leads to a minimum thermal excitation, and the extent of diffusion of alloying elements is limited. Hence, both shear strength and tensile strength become poor. With an increase in the joining temperature, the bond strength increases and attains its maximum value. This temperature promotes the mass transfer of the alloying elements across the

interface, which is responsible for the increase in the volume fraction of reaction products; hence, it causes more embrittlement of the joints with respect to the couples processed at 850 °C. However, plastic collapse of the mating surface asperities leads to intimate contact, which counterbalances the embrittlement phenomena due to intermetallic phases; the bond strength naturally increases. Beyond 900 °C diffusion bonding temperature, the width of intermetallics (Table IV) noticeably increases and the embrittlement effect compensates the effect due to the better plastic collapse of mating surfaces. So, the bond strength gradually drops and attains the lowest value at 1000 °C processing temperature (tensile and shear strengths are ~226 and ~132 MPa, respectively). The total width of intermetallic compounds formed at the SS-Cu interface at 1000 °C is 4 times larger than the total width of the intermetallic compounds for the samples processed at 900 °C and 2 times larger than the width of the intermetallics of the sample processed at 950 °C.

Figure 7 shows the change in mechanical properties of the diffusion-bonded joints with the variation in bonding time at 900 °C. For a 30-minute bonding time, both tensile and shear strength are minimum due to insufficient bonding time and result in the incomplete plastic collapse of mating surface asperities. With the rise in diffusion bonding time from 30 to 60 minutes, both tensile (~322 MPa) and shear (~254 MPa) strengths are increased and attain maximum values. At this bonding
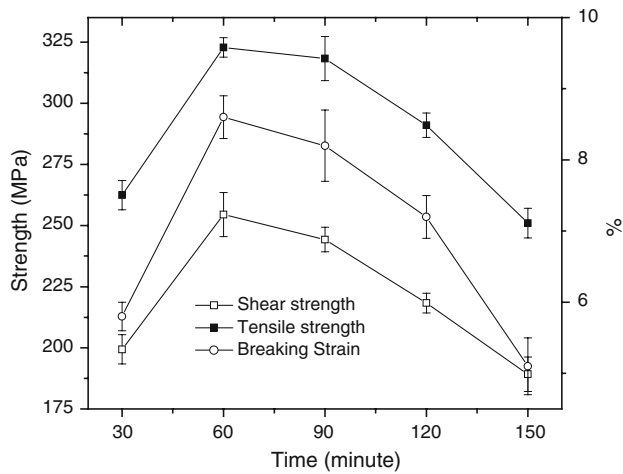
Fig. 7—Mechanical properties of the bonded joints processed at 900 °C temperature.

Fig. 8—Microhardness of the bonded joints at various process parameters at SS-Cu interface.

time, the plastic collapse of mating surfaces is increased as compared to lower bonding time and also promotes the atomic diffusivity of the chemical species, which in turn is accountable for the increase in the width of reaction products (Table V). With an increase in the bonding time to 90 minutes, the bond strength decreases marginally due to the marginal increase in the thickness of intermetallics. However, a further increase in the bonding time leads to a decrease in the bond strength due to the increase in the width of Fe-Ti base intermetallics at the SS-Cu interface, and bond strength attains the lowest tensile strength (~251 MPa) and shear strength (~189 MPa) values when diffusion bonding is processed for 150 minutes. The total width of intermetallic compounds for 150 minutes at the SS-Cu interface is 5 times larger than the total width of the intermetallic compounds for the samples processed for 60 minutes and 3 times larger than that of the sample processed for 120 minutes.

Figure 8 shows the microhardness of the bonded joints at the SS-Cu interface. It can be seen that the hardness of the interface is higher than that of the base material. The maximum hardness value is achieved at the SS-Cu interface due to the presence of brittle intermetallic phases at the Cu-SS interface. At the Cu-Ti interface, hardness values of the bright and dark region are 540 ± 15 HV and 290 ± 17 HV, when processed at 900 °C to 1000 °C for 60 minutes and at 900 °C for 60 to 150 minutes, respectively.

The fracture morphology of the bonded assemblies is shown in Figure 9. At 850 °C for 60 minutes, the fracture surfaces are basically featureless (Figure 9(a)). The dark area indicates the presence of voids. These irregularly shaped voids are generated presumably due to the lack of coalescence of the mating surfaces and encourage the failure under the load. However, the volume fraction of the dark area reduces with an increase in bonding temperature and time due to the better contact between mating surfaces. The area consists of a bright region and a deep-shaded region. The average composition of this area is Fe(~54.6 to 56.6),
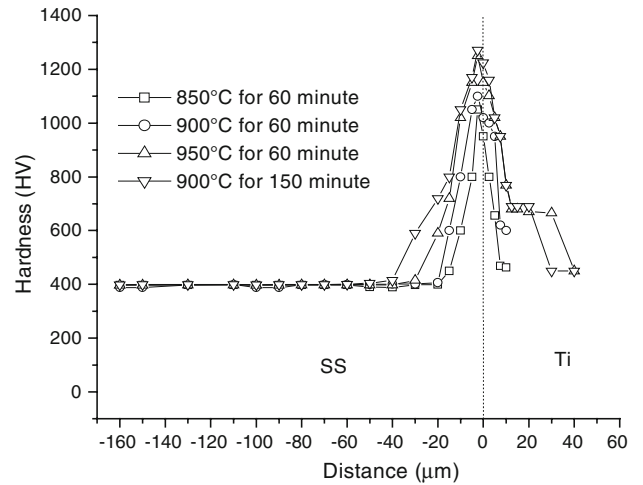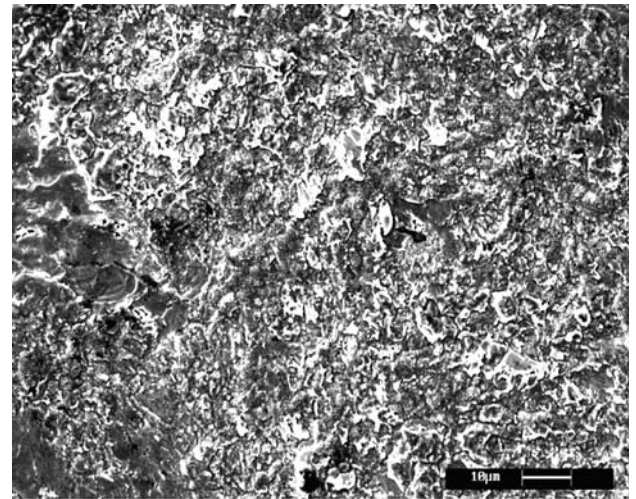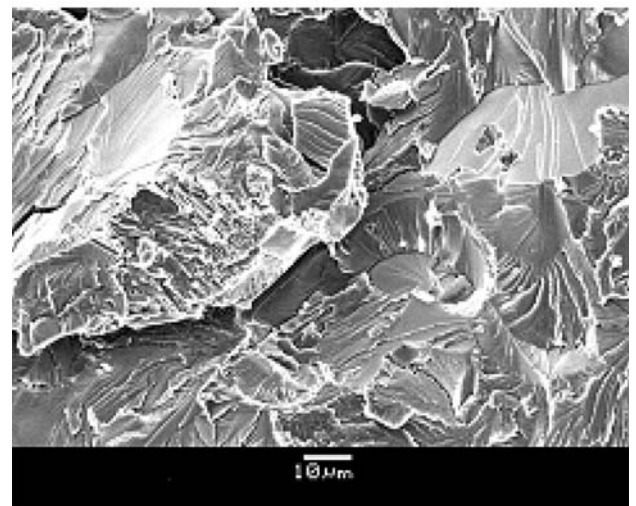

Fig. 9—Fracture surfaces of the bonded assembly processed (a) at 850 °C for 60 min, SS side; and (b) at 900 °C for 150 min, SS side.

Cr(26.1 to 28.7), Ti(12.4 to 14.2) along with a small amount of Cu(~0.7 to 1.1), and Ni(bal). So both areas indicate the presence of the α-Fe + λ phase mixture.

At 900 °C for 150 minutes of processing time, the fracture surface (Figure 9(b)) clearly indicates the brittle nature of the transition joint by the presence of cleavage planes with different alignments. The river pattern differs from grain to grain. The shaded matrix and bright lines of the river pattern have been noticed in the fracture. Both the shaded matrix and the bright line contain Fe(~35.6 to 36.1), Cr(~11.3 to 11.6), Ti(~47.6 to 49.2), Ni(~3.2 to 3.6), and Cu(bal.); hence, this area is the phase mixture of λ + FeTi + β-Ti.

IV. SUMMARY AND CONCLUSIONS

The diffusion bonding of the commercially pure Ti | Cu interlayer | 304 stainless steel was carried out at 850 °C to 1000 °C in steps of 50 °C for 60 minutes and 900 °C for 30 to 150 minutes in steps of 30 minutes under the compressive stress of 3 MPa in vacuum. The characterization of the diffusion-bonded joints reveals the following.

1. Optical micrographs indicate the greater diffusional distance of Cu in titanium than that of Cu in stainless steel. The SEM-BSE images exhibit the formation of a few of Cu-Ti and Fe-Cu-Ti base ternary products in the diffusion interfaces at the joining temperature of 850 °C for 60 and 30 minutes and 900 °C for 60 minutes, whereas, with the increase in bonding temperature and time, Fe-Cu-Ti and Cu-Ti base intermetallic phases are not formed at the diffusion interfaces.
2. The maximum bond strength (tensile strength ~322 MPa and shear strength ~254 MPa) and ductility (~8.5 pct) have been obtained for the diffusion-bonded joint processed at 900 °C for 60 minutes due to the better coalescence of mating surfaces and the finer width of Fe-Ti base intermetallics. With the rise in the joining temperature and

time, the bond strength gradually drops due to the increase in the width of the intermetallic phases.
3. The microhardness test across the joint interface indicates that the microhardness in the joint interface is greater than the base materials.
4. The fracture surface at 850 °C for 60 minutes is basically featureless; however, at 900 °C for 150 minutes, the existence of a cleavage pattern indicates the brittle nature of the joints. For all processing temperatures and times, failure takes place through the SS-Cu interface.

REFERENCES

1. X. Changqing and J. Zhangpeng: *J. Less Common Met.*, 1990, vol. 162, pp. 315–22.
2. K. Bhanumurthy and G.B. Kale: *J. Mater. Sci. Lett.*, 1993, vol. 12, pp. 1879–81.
3. G. Can and M. Kocak: *Int. Mater. Rev.*, 1998, vol. 43, pp. 1–44.
4. A. Fuji, K. Ameyama, and T.H. North: *J. Mater. Sci.*, 1996, vol. 31, pp. 819–27.
5. H. Kato, S. Abe, and T. Tomizawa: *J. Mater. Sci.*, 1997, vol. 32, pp. 5225–32.
6. B. Aleman, I. Guitterrez, and J.J. Urcola: *Mater. Sci. Technol.*, 1993, vol. 36, pp. 509–15.
7. M. Ghosh, K. Bhanumurthy, G.B. Kale, and S. Chatterjee: *J. Nucl. Mater.*, 2003, vol. 322, pp. 235–40.
8. T.B. Massalski: *Binary Alloy Phase Diagrams*, 2nd ed., ASM INTERNATIONAL, Materials Park, OH, 1990, p. 1783.
9. M. Eroglu, T.I. Khan, and N. Orhan: *Mater. Sci. Technol.*, 2002, vol. 18, pp. 68–72.
10. S. Kundu, S. Chatterjee, D. Olson, and B. Mishra: *Mater. Trans.*, 2007, vol. 38A, pp. 2053–60.
11. V. Raghavan: *Phase Diagrams of Ternary Iron Alloys*, ASM INTERNATIONAL, Metals Park, OH, 1987, vol. 1, p. 43.
12. V. Raghavan: *J. Phase Equilib.*, 2002, vol. 23, pp. 172–74.
13. J.A. van Beek, A.A. Kodentsov, and F.J.J. van Loo: *J. Alloys Compd.*, 1995, vol. 217, pp. 97–103.
14. N. Orhan, M. Aksoy, and M. Eroglu: *Mater. Sci. Eng.*, 1999, vol. A271, pp. 458–68.
15. S. Hinotani and Y. Ohmori: *Trans. Jpn. Inst. Met.*, 1988, vol. 29, pp. 116–24.
16. G.B. Kale, R.V. Patil, and P.S. Gande: *J. Nucl. Mater.*, 1998, vol. 257, pp. 44–50.